Multivalley optical switching in germanium

Junjun Jia[*]
Global Center for Science and Engineering (GCSE), Faculty of Science and Engineering, Waseda University, 3-4-1 Okubo, Shinjuku, Tokyo 169-8555, Japan

Hossam A. Almossalami and Hui Ye[†]
College of Optical Science and Engineering, Zhejiang University, Hangzhou 310027, China

Naoomi Yamada
Department of Applied Chemistry, Chubu University, Kasugai, Aichi 487-8501, Japan

Takashi Yagi
National Metrology Institute of Japan (NMIJ), National Institute of Advanced Industrial Science and Technology (AIST), Central 5, 1-1-1 Higashi, Tsukuba, Ibaraki 305-8565, Japan

(Received 2 September 2024; revised 26 November 2024; accepted 4 February 2025; published 24 February 2025)

Multicolored optical switching phenomena are crucial for a broad range of applications, such as telecommunications and optical computing. However, most materials typically exhibit single-colored optical nonlinearity under intense laser illumination. Herein, our femtosecond time-resolved transient transmission measurements reveal the coexistence of the transient Pauli blocking effect in both the Γ and *L* valleys following intense optical excitation in Ge films, demonstrating their feasibility as multicolored optical switching materials based on multivalley scattering. Additionally, a split-off energy of 240 meV at the *L* point, attributed to the spin-orbit coupling effect, is directly observed from time-resolved transient transmission spectra. Based on an accurately calculated band structure, a scheme has been developed to interpret pump-probe transient transmission traces, effectively avoiding overinterpretation of overlapping transient signals caused by multiple-transition pathways. Furthermore, analysis of transmission transients using a three-level model indicates that the intervalley scattering time between the Γ and *L* valleys is within 196 fs, and the intravalley scattering time is within 1.10 ps in the Γ valley, highlighting the potential for achieving an ultrafast multicolored optical switching device for key applications in multiband communications and optical computing.

DOI: 10.1103/PhysRevApplied.23.024060

I. INTRODUCTION

When a semiconductor material is irradiated by an intense laser with excitation energy larger than its band gap [1], optical switching can occur, making the material less absorptive and potentially changing from an opaque state to a transparent one within a specific wavelength region on ultrafast timescales, i.e., femtoseconds to nanoseconds [2]. Such phenomena have attracted significant attention for the development of optical switching devices in integrated photonics compatible with Si-technology-based optical communications owing to their ultrafast response time of down to several tens of femtoseconds [1,3], which are not achievable through conventional switching methods based on the resistive-capacitive delays of electronic circuits.

From the perspective of solid-state physics, when a large number of valence electrons are excited and injected into the conduction band after intense laser excitation, they scatter among themselves (electron-electron scattering) [4], with acoustic or optical phonons (electron-phonon scattering [5,6]), and with the remaining holes in the valence band (electron-hole scattering [7]). These electrons then relax to the bottom of the conduction band as thermalized electrons. Due to the Pauli blocking effect [8], the transient occupation of the thermalized electrons in the conduction band allows incident light to pass through the material, a phenomenon known as optical switching or optical bleaching [1]. The ultrafast response of such optical switching is typically constrained by the relaxation mechanisms of excited carriers, and largely depends on the electronic and phonon band structures of the semiconductor material. However, the complicated interplay between excited carriers and band structures often hinders the understanding required for utilizing such ultrafast optical switching, necessitating continued experimental and theoretical investigations.

[*]Contact author: jia@aoni.waseda.jp
[†]Contact author: huiye@zju.edu.cn

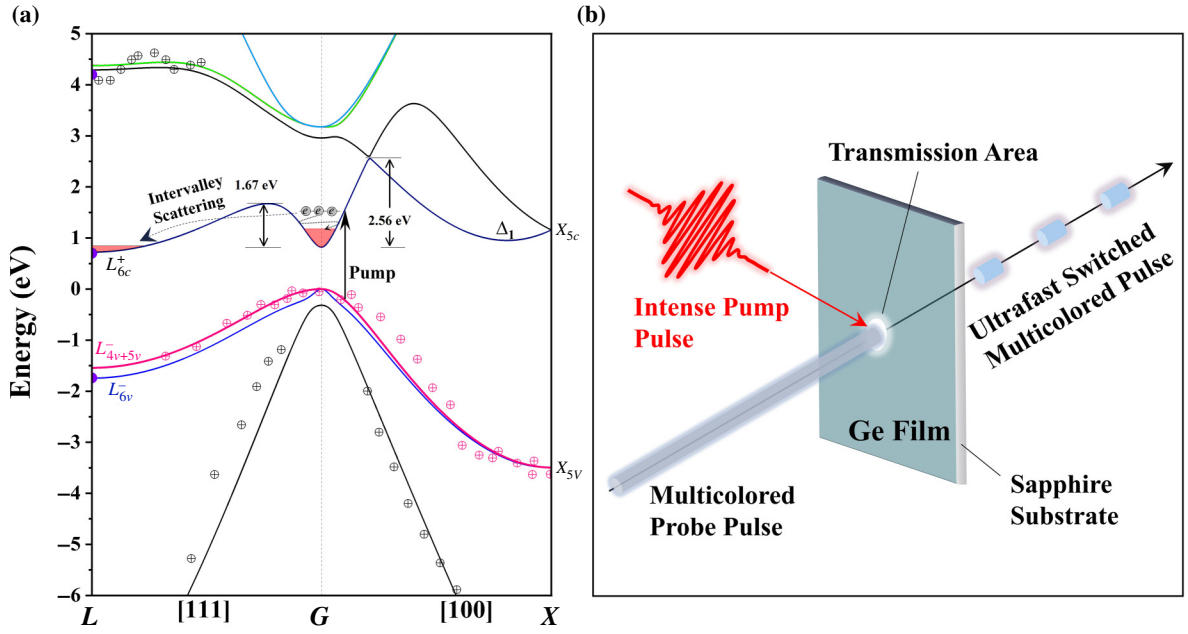

FIG. 1. (a) Calculated electronic band structure (solid lines) with spin-orbit coupling for diamond-structured Ge, compared with the experiments (solid half circles and circled plus) from angle-resolved photoemission and inverse photoemission measurements [24,25], where the valence-band maximum is set to zero. Note that the shaded regions show electronic occupation in the Γ and *L* valleys due to carrier injection, and the states at the high-symmetry points of the Brillouin zone are labeled according to the double-group notation of Koster *et al.* [26]. (b) Schematic representation of a multivalley optical switching device, wherein the switching material (Ge film) reversibly changes from an opaque state to a transparent one for specific wavelengths due to the Pauli blocking effect in both Γ and *L* valleys, triggered by intense laser irradiation. This optical switching mechanism can be examined using the pump-probe transient transmission measurements.

Ultrafast optical switching has been well observed in direct-band-gap materials, such as InN [1,9]. Femtosecond time-resolved pump-probe transient transmission measurements have demonstrated that the thermalized electrons follow a hot Fermi-Dirac distribution, and subsequently recombine with holes within several hundreds of picoseconds in InN films [1,10], enabling the possibility of ultrafast optical switching. In contrast, utilizing multivalley semiconductors for ultrafast optical switching has been less explored, possibly because the coexistence of direct and indirect valleys complicates the understanding of carrier thermalization and recombination. Intuitively, for multivalley semiconductors, excited electrons may be simultaneously distributed across different valleys due to intervalley scatterings [4,11], thereby opening the possibility of achieving multivalley optical switching from the aspect of Pauli blocking. This may even allow for optical switching at multiple distinct wavelengths, making multicolored switching devices feasible.

Herein, diamond-structured Ge, a traditional semiconductor material with a multivalley band structure, was subjected to intense laser irradiation to study its ultrafast carrier dynamics in different valleys and to evaluate the feasibility of multivalley optical switching, with the aim of achieving a multicolored optical switching device. The conduction band of bulk Ge consists of one Γ valley, four *L* valleys, and six *X* valleys. It has a direct band gap of 0.80 eV at the Γ point [12], and its indirect minimum at the *L* point is only 140 meV below the direct minimum [13]. The energy separation for direct transitions at the *L* point has been established to be approximately 2.11 eV at room temperature [14,15]. Recent experiments have also observed the existence of Pauli blocking for direct transitions at the *L* point in highly *n*-type doped Ge [16]. These properties make Ge a more promising candidate for a multicolored optical switching material. For example, when both Γ and *L* valleys are simultaneously filled with thermalized electrons following carrier injection and subsequent intervalley scatterings, as shown in Fig. 1(a), visible ($\sim$ 2.11 eV) and infrared ($\sim$ 0.80 eV) light can transiently pass through the sample due to the Pauli blocking effect.

A femtosecond time-resolved pump-probe transient transmission measurement system was developed to investigate multivalley optical switching phenomena, ranging from the infrared to the visible region in the Ge film, triggered by intense laser irradiation, as illustrated in Fig. 1(b). A set of three-level rate equations, incorporating multivalley scatterings, was constructed to model the measured

transient transmission traces. Using these rate equations, we successfully deconvoluted the temporal distributions of electronic occupation in different valleys in Ge, extracted inter- and intravalley scattering probabilities from the transient transmission traces, and demonstrated controllable multicolored optical switching with picosecond duration and >15% magnitude in the multivalley Ge semiconductor. These new findings also provide a framework for interpreting previous reports on the $\Gamma \rightarrow L$ intervalley scattering times measured by using other methods.

II. EXPERIMENTAL AND COMPUTATIONAL DETAILS

Considering potential applications of a Ge-based multivalley optical switching device in integrated silicon photonics [17], which is one of the emerging key technologies addressing the ever-growing demand for higher data rates and security due to internet traffic, a Ge-on-Si thin film was fabricated to examine multivalley optical switching. Molecular epitaxial evaporation, employing a low-high temperature two-step growth approach with cyclic annealing [17], was used to grow the polycrystalline Ge film on a 10-nm Si film coated on a *c*-sapphire substrate. The fabricated Ge sample (300 nm) is *p* type, with a hole concentration of 1.15×10^{18} cm^{-3} and a mobility of 78.1 cm^2/Vs. The film thickness, dielectric constants, and absorption coefficients were determined using a Jobin Yvon ellipsometer (UVISEL). The lattice constants, calculated from (222) and (110) XRD peaks, are 5.645 and 5.649 Å, respectively, which are in good agreement with the standard powder diffraction result (5.658 Å) [18].

Femtosecond time-resolved transient transmission measurements were performed to investigate ultrafast carrier dynamics based on the pump-probe technique. The Ge film was excited by a 140-fs Ti:S laser pulse with a repetition rate of 76 MHz at room temperature, in which the laser beam was split by a polarized beam splitter, with the majority of the power used to excite the sample (pumping at 1.55 eV) and the remaining power focused into the supercontinuum device (FemtoWHITE 800, NKT Photonics) for generating the probe light (400–1000 nm). Both pump and probe lights were focused on the sample surface using a 10× objective lens (Mitutoyo) with an incident angle of 90° relative to the sample surface, where the spot size of the 1.55-eV laser was 10.3 μm in diameter ($1/e^2$ diameter), as determined using the knife-edge technique. The transmitted probe light passed through a spectrometer and was then collimated to enter a Si photodetector (2107-FC, New Focus).

To explain the ultrafast dynamics of transient transmission, the photoexcited carrier density (N_e) was estimated using the calculation method developed by Menéndez *et al.* [19], which accounted for the lateral diffusion of excited electrons during pumping. In the calculation, the room-temperature average carrier lifetime, carrier-diffusion coefficient, and surface-recombination velocity were set to 0.9 ms [19], 53 cm^2/s [20], and 100 cm/s [21], respectively. For a pumping power of 240 mW at 1.55 eV, the photoexcited carrier density was estimated to be 2.99×10^{18} cm^{-3}, where the reflectance and absorption coefficients used, measured using a UV-vis spectrophotometer (UV-3600iPlus, Shimadzu), were 0.445 and 48 548 cm^{-1}, respectively.

Density-functional-theory (DFT) calculations were performed using the Vienna *ab initio* simulation package [22] with the projector-augmented-wave method [23]. The experimentally measured lattice constant with fixed fractional coordinates was used to calculate the band structure of Ge using the Heyd-Scuseria-Ernzerhof (HSE06) hybrid exchange-correlation functional with a plane-wave cutoff of 450 eV, where the spin-orbit coupling effect was also included to accurately represent the splitting of the valence bands. Note that fixing fractional coordinates ensures that the symmetry of the unit cell for diamond-structured Ge remains unchanged.

III. RESULTS AND DISCUSSION

To interpret the observed experimental results, we first calculated the band structure of diamond-structured Ge with a lattice constant of 5.645 Å by using the HSE06 functional, taking into account the spin-orbit coupling effect, as shown in Fig. 1(a). Over a wide energy range, the DFT band structure agrees well with the photoemission and inverse photoemission experimental data [24,25]. The calculated direct gap is 0.82 eV, which is in good agreement with the experimental values of 0.81 eV at room temperature [12]. The calculated indirect gap is 0.72 eV at the L_{6c}^{+} point, which is consistent with the value (0.7 eV) from the inverse photoemission experiment [24] and slightly larger than the well-established value of 0.66 eV obtained from optical measurements [13]. The energy of the Δ_1 conduction-band minimum is 0.95 eV above the valence-band maximum, and the energy separation between X_{5c} and X_{5v} is 4.65 eV, which is larger than the reported experimental value (4.36–4.38 eV at 300 K) determined using spectroscopic ellipsometry [14,15]. The spin-orbit coupling causes the splitting of the valence bands, and the energy separations for the top valence band are calculated to be 0.32 and 0.20 eV at the Γ and L points, which are in good agreement with experimental values of 0.30 and 0.23 eV, respectively [15,27]. The energy at L_{6v}^{-} is 1.74 eV below the valence-band maximum, consistent with the reported value (1.74 eV) from the angle-resolved photoemission measurement [24,25]. The intervalley energies along the [111] and [100] directions are 1.67 and 2.56 eV, respectively.

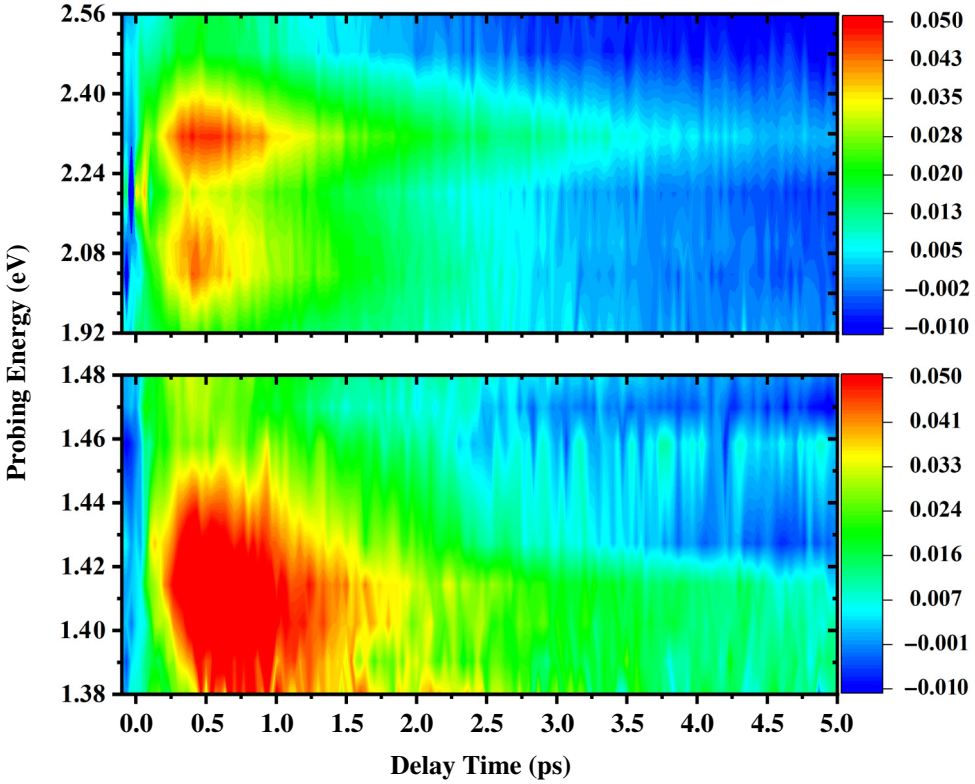

FIG. 2. Time-resolved transient transmission spectra measured at a pumping fluence of 7.58×10^{-3} J/cm^2. Herein, a pump laser with an energy of 1.55 eV was used, and a pump laser with an energy of 1.55 eV was used, and the transient transmission spectra were measured using a probe laser with energies ranging from 1.38 to 2.56 eV.

Figure 2 shows the transient transmission, probing from 1.38 to 2.56 eV, under optical excitation at 1.55 eV with a pumping fluence of 7.58×10^{-3} J/cm^2, where the transient transmission signal is defined as $dT/T = [T(t) - T(0)]/T(0)$ with the transient transmission, $T(t)$, and the static transmission, $T(0)$. The overall temporal response shows three notable switching regions, offering the possibility for use as a multicolored optical switching material, where multicolor refers to three distinct wavelengths. The most prominent switching region is centered at approximately 1.41 eV, while two additional switching regions are located at around 2.08 and 2.32 eV. These switching states can be explained in terms of Pauli blocking, which causes a change from an opaque state to a transparent state. Simply speaking, the probing level in the conduction band becomes occupied by a large number of excited electrons following intense pumping, allowing the probing pulse to pass through the excited sample, as clarified by the Burstein-Moss effect [8]. It is worth noting that, even if all the excited electrons (2.99×10^{18} cm^{-3}) are injected into the conduction band simultaneously without considering carrier depopulation, their collective motion has a negligible effect on the visible transmittance from 1.92 to 2.56 eV, as calculated by the classical Drude model.

Understanding the observed optical switching requires a detailed examination of ultrafast carrier dynamics following intense excitation. Generally, for a direct-band-gap material, excited electrons typically relax to lower energy levels in the conduction band through the electron-phonon or electron-electron scattering mechanisms shortly after pumping, a process commonly referred to as thermalization [1,5–7,28]. This relaxation results in a transient occupation of thermalized electrons in the Γ valley, thereby initiating optical switching. Considering Ge as a multivalley semiconductor, in addition to the relaxation of electrons within the Γ valley, a portion of the excited electrons are scattered into the L valley, contributing to optical switching in the L valley.

Based on the above physical picture, the strongest optical switching, centered at 1.41 eV, is attributed to the direct optical transition, due to the transient occupation of thermalized electrons in the Γ valley. The optical switching observed around 2.32 eV is attributed to the optical transition from L_{6v}^{-} to L_{6c}^{+}, while the weak one near 2.08 eV is considered to be due to transitions between L_{4v+5v}^{-} and L_{6c}^{+}. The energy separation (224 meV) between two switching centers is close to experimentally reported values (170–240 meV) at the L point, as shown in Table I, and

TABLE I. Calculated splitting energies and gap energies at the L point in Ge, obtained from the DFT-HSE06 calculations with a room-temperature lattice constant of 5.645 Å. Experimental values measured around room temperature are provided for comparison.

	Splitting (meV)		Gaps at L (eV)	
	$\Delta_{SO}(\Gamma)$	$\Delta_{SO}(L)$	$L^-_{4v+5v} \rightarrow L^+_{6c}$	$L^-_{6v} \rightarrow L^+_{6c}$
Present Calc[a]	320	200	2.25	2.45
Calc[b]	290	200	2.08	2.27
Expt.[c]	–	170	2.09	2.26
Expt.[d]	–	200	2.15	2.35
Expt.[e]	–	180	2.134	2.314
Expt.[f]	–	200–240	2.11–2.14	2.33–2.36
Expt.[g]	–	210	2.115	2.325
Expt.[h]	–	187	2.111	2.298
Expt.[i]	–	196	2.107	2.303
Expt.[j]	–	198	2.105	2.303
Expt.[k]	–	200	2.1	2.3
Expt.[l]	–	200	2.09	2.29
Expt.[m]	–	201	2.065	2.266
Expt.[n]	290	190	2.05	2.24
Expt.[o]	286	200	2.11	2.31
Present Expt.[p]	–	224	2.08	2.32

[a]Our calculation by using the HSE06 functional.
[b]Theoretical calculation by Fourier expansion [29].
[c]Electroreflectance measured at room temperature [30].
[d]Absorption experiments at 295 K [31].
[e]Thermoabsorption experiments at 295 K [32].
[f]Electroreflectance measured at room temperature for n and p types with different carrier densities [33].
[g]Electroreflectance measurements at room temperature [34].
[h]Ellipsometry measurements at room temperature [14].
[i]Electroreflectance measured at room temperature [35].
[j]Electroreflectance measurements at room temperature [36].
[k]Reflectance measurements at 300 K [37].
[l]Piezoreflectance measurements at room temperature [38].
[m]Electroreflectance measured at room temperature [39].
[n]Electroreflectance measured at room temperature [40].
[o]Data were extrapolated at 300 K based on the temperature dependence of interband critical point energies obtained from ellipsometry measurements [15].
[p]Present pump-probe experimental work.

agrees with the present DFT calculation. To the best of our knowledge, the simultaneous occupation of thermalized electrons in the Γ and L valleys has not been previously reported.

A. Multiple-transition pathways

Figure 3(a) shows three transient transmittance measurements at various probing energies under a pumping energy of 1.55 eV. With reference to the band dispersion shown in Fig. 1(a), the optical switching detected at a probing energy of 2.21 eV is directly attributed to transient electronic occupation in the L valley, whereas those measured at probing energies of 1.48 and 1.73 eV reflect transient Pauli blocking in the Γ valley. Importantly, the direct transition pathways can originate from the heavy-hole (HH), light-hole (LH), and split-off (SO) bands for both pump and probe pulses, as indicated by the dashed arrows in Fig. 3(b). By analyzing the energy separation between the conduction and valence bands, the highest excitation level is determined to be 1.45 eV above the valence-band maximum for a pumping energy of 1.55 eV. The results of this analysis suggest that direct transitions from HH, LH, and SO bands at a probing energy of 1.48 eV can capture electronic occupation at different energy levels below 1.45 eV in the Γ valley, which almost ranges from 0.80 to 1.45 eV, as shown in Fig. 3(b). Such multiple-transition pathways cause an overlap of the dT/T signals, and make data interpretation challenging. Due to the lack of detailed information on the nonthermal and thermalized electrons following excitation, a quantitative evaluation of contributions of transitions from different valence bands to the dT/T signal is hardly possible.

On the other hand, at a probing energy of 1.73 eV, only two direct transitions from the SO bands to the conduction band are allowed below the highest excitation energy of 1.45 eV, as shown in Fig. 3(b). The energy separation between two probing levels is 30 meV. This small separation allows us to approximate two probing levels as a discrete level (a single-transition pathway) and then to analyze the temporal behavior of transient electronic occupation in the Γ valley. In contrast, because the dispersion of the top valence band (L^-_{4v+5v}) is fairly flat around the L point, a single direct transition pathway is sufficient to explain the experimental data.

It is worth noting that the effects of band-gap renormalization caused by laser heating and carrier-carrier interactions on the band structure of Ge are neglected in the above discussions. Band-gap normalization is typically induced by two factors: (1) an increase in lattice temperature, and (2) carrier-carrier interactions between the massive excited carriers following intense pumping. In the pump-probe measurement, continuous pumping leads to a rise in lattice temperature, which can be estimated by the Cahill formula [41], namely, $\Delta T = \alpha p/2\sqrt{\pi} w_0 \kappa$, where α is the absorption coefficient at 800 nm, p is the pump power, w_0 is the $1/e^2$ radius of the pump beam, and $\kappa = 39$ W/mK is the thermal conductivity of the Al_2O_3 substrate [1]. The estimated temperature rise is 108 K. This temperature rise can result in band-gap shrinkage due to thermal expansion. The indirect band gap of Ge as a function of lattice temperature can be expressed using Varshni's empirical formula [14]:

$$E_g(\theta) = E_g(0) - \frac{\alpha T^2}{T + \beta}, \tag{1}$$

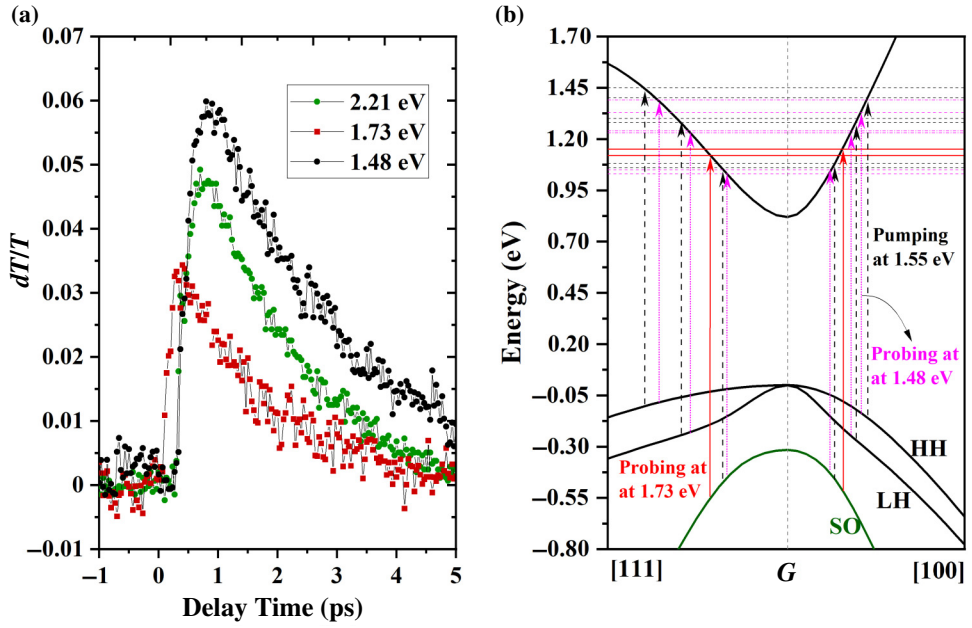

FIG. 3. (a) Transient transmission traces detected at different probing energies, where the pumping energy is 1.55 eV and its fluence is 7.58×10^{-3} J/cm^2. (b) Multiple vertical transition pathways occur under a pumping energy of 1.55 eV (dashed arrows) and probing energy of 1.48 eV (dotted arrows). In contrast, two closely spaced vertical transition levels at a probing energy of 1.73 eV (solid arrows) are considered to be a single-transition pathway. Note that the optical transition energies between the two bands were calculated based on the band dispersion obtained from the DFT-HSE06 calculations with the spin-orbit coupling effect.

where $E_g(0) = 0.741$ eV is the indirect band gap of Ge at 0 K, $\alpha = 0.456$ meV K^{-1}, and $\beta = 210$ K [14]. A simple calculation shows that the band-gap shrinkage is only 40 meV compared to the value at room temperature. On the other hand, carrier-carrier interactions are reported to induce a band-gap shrinkage of only approximately 10 meV, when the excited-electron concentration reaches 3.50×10^{20} cm^{-3} [42], which is significantly higher than that in the present experiment.

B. Modeling of transmission transients

Based on the discussion above, selecting a suitable probing energy in the pump–probe-based transient transmission measurements can minimize the influence of multiple-transition pathways on the dT/T signals and enable precise analysis of temporal evolution of electronic occupation at specific energy levels. For a multivalley semiconductor, this approach also enables the detection of the temporal evolution of electronic occupation at specific levels in different valleys by using multiple probing lasers simultaneously, thereby making the analysis of multivalley scattering possible.

In the case of Ge, after pumping, excited electrons rapidly thermalize from the pumping level to the Γ and L valleys, forming two distinct hot Fermi distributions. From the aspect of pump-probe measurements, the temporal evolution of electronic occupations at specific levels in both the Γ and L valleys can be detected by suitable probing energies. In the Γ valley, thermalized electrons occupying the probing level may originate from the pumping level through thermalization, scatter to the L valley, or depopulate from the Γ valley. On the other hand, in the L valley, thermalized electrons occupying the probing level may originate from the Γ valley, backscatter to the Γ valley through electron-optical phonon scattering [19], or depopulate from the L valley. Figure 4(a) illustrates these possible evolutions, where Γ and L conduction-band states are treated as continuous, except for the pumping level. This is because the highest pumping level under 1.55-eV excitation is 0.65 eV above the Γ minimum, as shown in Fig. 3(b), which is significantly higher than the maximum Fermi-level shift caused by carrier injection, and thus, the pumping level is regarded as a discrete energy level in our experiment. To describe these situations, the following three-level rate equations have been developed:

$$\frac{dN_P}{dt} = G(t) - k_\Gamma N_P, \tag{2}$$

$$\frac{dN_\Gamma}{dt} = k_\Gamma N_P + k_{L\Gamma} N_L - k_{\Gamma L} N_\Gamma - k_{D\Gamma} N_\Gamma, \tag{3}$$

$$\frac{dN_L}{dt} = k_{\Gamma L} N_\Gamma - k_{L\Gamma} N_L - k_{DL} N_L, \tag{4}$$

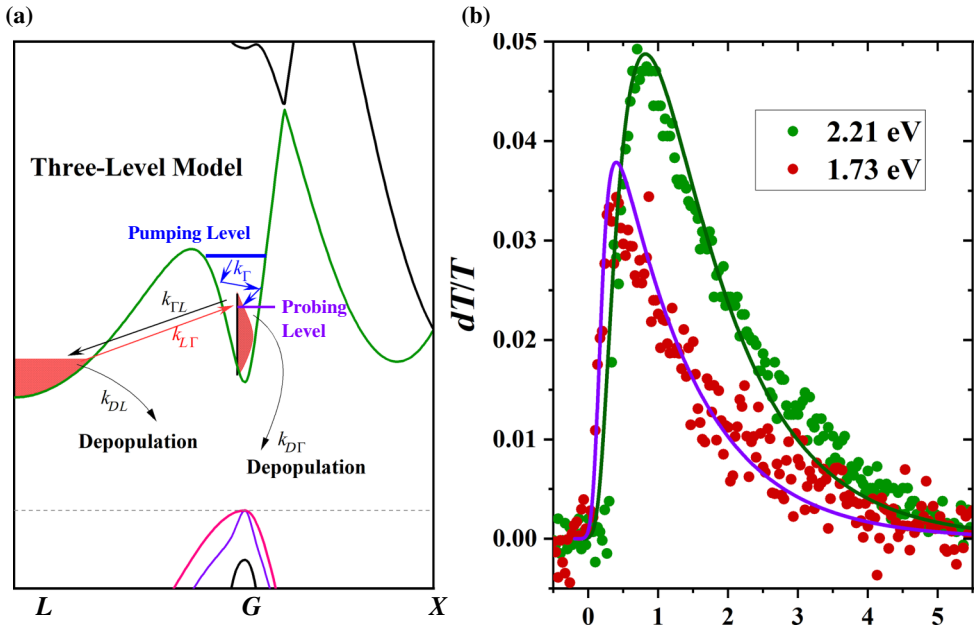

FIG. 4. (a) Schematic diagram of a three-level model describing the intravalley and intervalley carrier relaxations, as well as carrier depopulation from the Γ and L valleys following optical excitation. Dashed line represents the valence-band maximum. (b) Numerical fits of measured transient transmission traces to the three-level model using the Runge-Kutta method, where the scatter points represent experimental data. Vertical transitions of 1.73 and 2.21 eV are considered to be two single-transition pathways in the Γ and L valleys, respectively.

where N_P is the photoexcited-electron concentration at the pumping level; N_Γ and N_L are the thermalized electron concentrations in the Γ and L valleys, respectively. The intravalley scattering rate in the Γ valley is k_Γ, and the intervalley scattering rates between the Γ and L valleys are $k_{\Gamma L}$ and $k_{L\Gamma}$, respectively. For completeness, the depopulation rates in the Γ and L valleys are considered as $k_{D\Gamma}$ and k_{DL} [43], respectively, due to recombination or other effects [44,45]. The term $G(t) = N_e\sqrt{2/\pi\tau_p^2}\exp[-2(t/\tau_p)^2]$ stands for carrier generation by a Gaussian optical pulse, where τ_p is the pulse width.

Recent studies indicate that intervalley scattering between the Γ and L valleys in Ge can be facilitated by forbidden TA and LO phonon modes, which dominate indirect absorption and emission near room temperature [19]. Specifically, although the electron-phonon coupling exactly at the Γ and L points is forbidden by symmetry for TA and LO phonon modes [46], it becomes allowed for states slightly off these high-symmetry points [19]. Furthermore, the ratio of phonon-assisted intervalley scattering to backscattering from the Γ to L valley can be expressed as [47,48]

$$\frac{k_{\Gamma L}}{k_{L\Gamma}} \propto \frac{D_L}{D_\Gamma}\left(\frac{m_L^*}{m_\Gamma^*}\right)^{3/2}, \tag{5}$$

where $D_L = 4$ and $D_\Gamma = 1$ represent the degeneracies of the L and Γ valleys, respectively. The effective masses of electrons are $m_L^* = 0.12m_e$ and $m_\Gamma^* = 0.04m_e$ at the L and Γ points, respectively, where m_e denotes the free-electron mass. As a result, the ratio $k_{\Gamma L}/k_{L\Gamma}$ is approximately 21, indicating that $L \to \Gamma$ backscattering is negligible. This conclusion is further supported by photoluminescence experiments [45].

To estimate intravalley and intervalley scattering times in Ge films, probing energies of 1.73 and 2.21 eV, corresponding to two single-optical-transition pathways in the Γ and L valleys, as discussed above, were selected to investigate the temporal evolution of electronic occupation in both valleys. Then, the rate equations (2)–(4) were used to fit their transient transmission traces by varying k_Γ, $k_{\Gamma L}$, $k_{D\Gamma}$, and k_{DL}. Figure 4(b) illustrates the best-fit curves for transient transmission traces probed at 1.73 and 2.21 eV. The fitting curves are in good agreement with experimental data. From the fits, the extracted lifetimes are $1/k_{\Gamma L} = 196$ fs, $1/k_\Gamma = 1100$ fs, $1/k_{DL} = 360$ fs, and $1/k_{D\Gamma} = 200$ fs.

The intervalley scattering time is estimated to be $1/k_{\Gamma L} = 196$ fs, which is in close agreement with the 165-fs value derived from the broadening of the interband critical point in the ellipsometry spectrum [15] and the 100-fs value determined using a four-wave mixing technique [49]. In the Ge/SiGe quantum well system, the intervalley scattering time is reported to be 185 fs [50]. Zhou *et al.*

also reported a fitted value of 230 fs for bulk Ge, extracted from a simple exponential fitting of the pump-probe transmission trace [28,51]. Notably, these intervalley scattering times are obviously smaller than the 1.2-ps experimental value obtained via time-resolved inelastic light scattering [52]. On the other hand, intravalley scattering was not accounted for in other studies. Our fitting reveals that the intravalley scattering time, $1/k_{\Gamma}$, is 1100 fs, and this timescale is primarily attributed to electron-phonon scattering rather than ultrafast electron-electron scattering, which typically occurs on a much shorter timescale of ≤ 100 fs [53]. Since intravalley optical-phonon scattering is symmetry forbidden in the Γ valley [54], this long intravalley scattering time can be attributed to scattering interactions between thermalized electrons and lower-energy acoustic phonons, which possibly originate from anharmonic decay of optical phonons [55,56] generated by intervalley scatterings. Moreover, the maximal fraction of electrons transferred to the L valley is estimated to be approximately 63%, indicating the feasibility of multicolored optical switching. This result is corroborated by other photoluminescence experiments, where indirect-gap emission from the L minimum is much stronger in bulk Ge samples [57], and the direct-gap emission in Ge films can be enhanced by optical excitation [45].

IV. CONCLUSIONS

We investigated the multivalley optical switching phenomenon in the Ge film under intense laser irradiation via femtosecond time-resolved transient transmission measurements. Ultrafast optical switching was observed in both the Γ and L valleys, suggesting the coexistence of intravalley and intervalley scatterings. Moreover, a split-off energy of 240 meV at the L point is directly observed in the time-resolved transient transmission spectra. Due to the complicated valence-band structure, the transient signal strongly depends on the exact region of the band structure involved. With reference to the band dispersion calculated using the HSE06 functional and spin-orbit coupling effect, we chose two suitable probing energies to minimize the overlap of transient signals due to multiple-transition pathways, thereby allowing accurate capture of transient electronic occupation in both the Γ and L valleys. By fitting the measured transient transmission traces with the three-level rate equations, the intravalley and intervalley scattering times were determined to be 196 and 1100 fs, respectively. Although the three-level rate equations are simple, they provide valuable insights into carrier-scattering mechanisms in multivalley semiconductors and help to avoid complications associated with more detailed calculations.

Overall, our experimental results highlight the potential of Ge as a multicolored optical switching material. The present study demonstrates the potential of polycrystalline Ge films for multivalley optical switching, and an epitaxial Ge film on the Si film or Si substrate [58] is expected to exhibit better performance. These findings lay a solid foundation for the development of novel multicolored optical switching devices in integrated photonics.

ACKNOWLEDGMENTS

J.J. acknowledges funding from a Waseda University Grant for Special Research Projects (Projects No. 2024C-181 and No. 2024R-030). J.J. also acknowledges funding from a JSPS KAKENHI Grant-in-Aid for Scientific Research (C) (Grant No. 20K05368).

J.J. conceptualized the study and performed the theoretical calculations. H.A. and H.Y. fabricated the p-type Ge film. N.Y. conducted transmittance and reflectance experiments. J.J. and T.Y. developed the pump-probe measurement system and collected the experimental data. J.J. provided the theoretical framework for data interpretation. J.J. wrote and revised the manuscript, and H.Y., N.Y., and T.Y. reviewed the manuscript.

The authors declare no competing interests.

DATA AVAILABILITY

The data supporting the findings of this study are available within the article. Numerical datasets and additional Python fitting programs can be obtained from the corresponding author upon reasonable request.

[1] J. Jia, T. Yagi, M. Mizutani, N. Yamada, and T. Makimoto, Revealing the simultaneous increase in transient transmission and reflectivity in InN, J. Appl. Phys. **132**, 165702 (2022).

[2] S. Saha, B. T. Diroll, M. G. Ozlu, S. N. Chowdhury, S. Peana, Z. Kudyshev, R. D. Schaller, Z. Jacob, V. M. Shalaev, A. V. Kildishev, and A. Boltasseva, Engineering the temporal dynamics of all-optical switching with fast and slow materials, Nat. Comm. **14**, 5877 (2023).

[3] G. Grinblat, M. P. Nielsen, P. Dichtl, Y. Li, R. F. Oulton, and S. A. Maier, Ultrafast sub–30-fs all-optical switching based on gallium phosphide, Sci. Adv. **5**, eaaw3262 (2019).

[4] M. A. Osman and D. K. Ferry, Monte Carlo investigation of the electron-hole-interaction effects on the ultrafast relaxation of hot photoexcited carriers in GaAs, Phys. Rev. B **36**, 6018 (1987).

[5] A. C. S. Algarte, Effect of free-carrier screening on the ultrafast relaxation kinetics in hot polar semiconductors, Phys. Rev. B **32**, 2388 (1985).

[6] W. Pötz and P. Kocevar, Electronic power transfer in pulsed laser excitation of polar semiconductors, Phys. Rev. B **28**, 7040 (1983).

[7] M. Asche and O. G. Sarbei, The role of electron-hole interaction in the cooling process of highly excited carriers, Phys. Status Solidi B **126**, 607 (1984).

[8] E. Burstein, Anomalous optical absorption limit in InSb, Phys. Rev. **93**, 632 (1954).; T. S. Moss, The interpretation of the properties of indium antimonide, Proc. Phys. Soc. Lond., Ser. B **67**, 775 (1954).

[9] V. Pačebutas, G. Aleksejenko, A. Krotkus, J. W. Ager III, W. Walukiewicz, H. Lu, and W. J. Schaff, Optical bleaching effect in InN epitaxial layers, Appl. Phys. Lett. **88**, 191109 (2006).

[10] T. Tsai, C. Chang, and S. Gwo, Ultrafast hot electron relaxation time anomaly in InN epitaxial films, Appl. Phys. Lett. **90**, 252111 (2007).

[11] V. G. Tyuterev, S. V. Obukhov, N. Vast, and J. Sjakste, *Ab initio* calculation of electron-phonon scattering time in germanium, Phys. Rev. B **84**, 035201 (2011).

[12] S. Zwerdling, B. Lax, L. M. Roth, and K. J. Button, Exciton and magneto-absorption of the direct and indirect transitions in germanium, Phys. Rev. **114**, 80 (1959).

[13] G. G. Macfarlane, T. P. McLean, J. E. Quarrington, and V. Roberts, Fine structure in the absorption-edge spectrum of Ge, Phys. Rev. **108**, 1377 (1957).

[14] L. Viña, S. Logothetidis, and M. Cardona, Temperature dependence of the dielectric function of germanium, Phys. Rev. B **30**, 1979 (1984).

[15] C. Emminger, F. Abadizaman, N. S. Samarasingha, T. E. Tiwald, and S. Zollner, Temperature dependent dielectric function and direct bandgap of Ge, J. Vac. Sci. Technol. B **38**, 012202 (2020).

[16] C. Xu, N. S. Fernando, S. Zollner, J. Kouvetakis, and J. Menéndez, Observation of phase-filling singularities in the optical dielectric function of highly doped *n*-type Ge, Phys. Rev. Lett. **118**, 267402 (2017).

[17] H. Ye and J. Yu, Germanium epitaxy on silicon, Sci. Technol. Adv. Mater. **15**, 024601 (2014).

[18] H. E. Swanson and E. Tatge, Standard x-ray diffraction powder patterns, Natl. Bur. Stand. (U. S.), Circ. **539**, 18 (1951).

[19] J. Menéndez, C. D. Poweleit, and S. E. Tilton, Temperature-dependent photoluminescence in Ge: Experiment and theory, Phys. Rev. B **101**, 195204 (2020).

[20] A. L. Smirl, S. C. Moss, and J. R. Lindle, Picosecond dynamics of high-density laser-induced transient plasma gratings in germanium, Phys. Rev. B **25**, 2645 (1982).

[21] B. P. Swain, H. Takato, and I. Sakata, Passivation of germanium surfaces by a quinhydrone–methanol solution treatment, Jpn. J. Appl. Phys. **50**, 071302 (2011).

[22] G. Kresse and J. Furthmüller, Efficient iterative schemes for *ab initio* total-energy calculations using a plane-wave basis set, Phys. Rev. B **54**, 11169 (1996).

[23] G. Kresse and D. Joubert, From ultrasoft pseudopotentials to the projector augmented-wave method, Phys. Rev. B **59**, 1758 (1999).

[24] D. Straub, L. Ley, and F. J. Himpsel, Inverse-photoemission study of unoccupied electronic states in Ge and Si: Bulk energy bands, Phys. Rev. B **33**, 2607 (1986).

[25] F. J. Himpsel, Inverse photoemission from semiconductors, Surf. Sci. Rep. **12**, 1 (1990).

[26] G. F. Koster, J. O. Dimmock, R. G. Wheeler, and H. Statz, *Properties of the Thirty-Two Point Groups* (M.I.T. Press, Cambridge, MA, 1963).

[27] D. E. Aspnes, Schottky-barrier electroreflectance of Ge: Nondegenerate and orbitally degenerate critical points, Phys. Rev. B **12**, 2297 (1975).

[28] X. Q. Zhou, H. M. van Driel, and G. Mak, Femtosecond kinetics of photoexcited carriers in germanium, Phys. Rev. B **50**, 5226 (1994).

[29] G. Dresselhaus and M. S. Dresselhaus, Fourier expansion for the electronic energy bands in silicon and germanium, Phys. Rev. **160**, 649 (1967).

[30] T. Nishino and Y. Hamakawa, Low temperature electroreflectance spectra of germanium in spectral region from 0.7 to 2.6 eV, J. Phys. Soc. Jpn. **26**, 403 (1969).

[31] M. Cardona and G. Harbeke, Absorption spectrum of germanium and zinc-blende-type materials at energies higher than the fundamental absorption edge, J. Appl. Phys. **34**, 813 (1963).

[32] F. R. Kessler and K. Dettmer, Separation of the e_1 and E_1 interband transitions near 2 eV in germanium by thermoabsorption, Phys. Status Solidi B **51**, 79 (1972).

[33] M. Cardona, K. L. Shaklee, and F. H. Pollak, Electroreflectance at a semiconductor-electrolyte interface, Phys. Rev. **154**, 696 (1967).

[34] K. L. Shaklee, F. H. Pollak, and M. Cardona, Electroreflectance at a semiconductor-electrolyte interface, Phys. Rev. Lett. **15**, 883 (1965).

[35] J. Humlíček, On the nature of E_1-transitions in germanium, Phys. Status Solidi B **86**, 303 (1978).

[36] D. E. Aspnes and J. E. Rowe, E_1 Transition in Ge: Two dimensional or three dimensional? Phys. Rev. B **7**, 887 (1973).

[37] H. Ehrenreich, H. R. Philipp, and J. C. Phillips, Interband transitions in groups 4, 3-5, and 2-6 semiconductors, Phys. Rev. Lett. **8**, 59 (1962).

[38] J. Takizawa, H. Fukutani, and G. Kuwabara, Piezoreflectance studies of GaP and Ge, J. Phys. Soc. Jpn. **35**, 543 (1973).

[39] S. Koeppen, P. Handler, and S. Jasperson, Parallel nature of the Λ_1–Λ_3 energy bands in germanium, Phys. Rev. Lett. **27**, 265 (1971).

[40] A. K. Ghosh, Electroreflectance spectra and band structure of germanium, Phys. Rev. **165**, 888 (1968).

[41] D. G. Cahill, Analysis of heat flow in layered structures for time-domain thermoreflectance, Rev. Sci. Instrum. **75**, 5119 (2004).

[42] M. Zürch, H.-T. Chang, L. J. Borja, P. M. Kraus, S. K. Cushing, A. Gandman, C. J. Kaplan, M. H. Oh, J. S. Prell, D. Prendergast, C. D. Pemmaraju, D. M. Neumark, and S. R. Leone, Direct and simultaneous observation of ultrafast electron and hole dynamics in germanium, Nat. Comm. **8**, 15734 (2017).

[43] C. J. Stanton and D. W. Bailey, Rate equations for the study of femtosecond intervalley scattering in compound semiconductors, Phys. Rev. B **45**, 8369 (1992).

[44] S. Tiwari, E. Kioupakis, J. Menéndez, and F. Giustino, Unified theory of optical absorption and luminescence including both direct and phonon-assisted processes, Phys. Rev. B **109**, 195127 (2024).

[45] G. Grzybowski, R. Roucka, J. Mathews, L. Jiang, R. T. Beeler, J. Kouvetakis, and J. Menéndez, Direct versus

indirect optical recombination in Ge films grown on Si substrates, Phys. Rev. B **84**, 205307 (2011).

[46] G. A. Thomas, E. I. Blount, and M. Capizzi, Indirect recombination mechanisms in germanium, Phys. Rev. B **19**, 702 (1979).

[47] C. Herring, Transport properties of a many-valley semiconductor, Bell Syst. Tech. J. **34**, 237 (1955).

[48] S. Marcinkevičius, T. K. Uždavinys, H. M. Foronda, D. A. Cohen, C. Weisbuch, and J. S. Speck, Intervalley energy of GaN conduction band measured by femtosecond pump-probe spectroscopy, Phys. Rev. B **94**, 235205 (2016).

[49] T. Rappen, U. Peter, M. Wegener, and W. Schäfer, Coherent dynamics of continuum and exciton states studied by spectrally resolved fs four-wave mixing, Phys. Rev. B **48**, 4879 (1993).

[50] S. A. Claussen, E. Tasyurek, J. E. Roth, and D. A. B. Miller, Measurement and modeling of ultrafast carrier dynamics and transport in germanium/silicon-germanium quantum wells, Opt. Express **18**, 25596 (2010).

[51] G. Mak and H. M. van Driel, Femtosecond transmission spectroscopy at the direct band edge of germanium, Phys. Rev. B **49**, 16817 (1994).

[52] K. Tanaka, H. Ohtake, and T. Suemoto, Determination of intervalley scattering time in germanium by subpicosecond time-resolved Raman spectroscopy, Phys. Rev. Lett. **71**, 1935 (1993).

[53] L. Rota, P. Lugli, T. Elsaesser, and J. Shah, Ultrafast thermalization of photoexcited carriers in polar semiconductors, Phys. Rev. B **47**, 4226 (1993).

[54] J. F. Young, K. Wan, and H. M. van Driel, Picosecond Raman scattering from non-equilibrium LO and TO phonons in germanium, Solid State Electron. **31**, 455 (1988).

[55] A. Debernardi, S. Baroni, and E. Molinari, Anharmonic phonon lifetimes in semiconductors from density-functional perturbation theory, Phys. Rev. Lett. **75**, 1819 (1995).

[56] A. Othonos, Probing ultrafast carrier and phonon dynamics in semiconductors, J. Appl. Phys. **83**, 1789 (1998).

[57] T. H. Cheng, C. Y. Ko, C. Y. Chen, K. L. Peng, G. L. Luo, C. W. Liu, and H. H. Tseng, Competitiveness between direct and indirect radiative transitions of Ge, Appl. Phys. Lett. **96**, 091105 (2010).

[58] E. Wangila, S. K. Saha, R. Kumar, A. Kuchuk, C. Gunder, S. Amoah, K. R. Khiangte, Z. Chen, S.-Q. Yu, and G. J. Salamo, Single crystalline Ge thin film growth on *c*-plane sapphire substrates by molecular beam epitaxy (MBE), CrystEngComm **24**, 4372 (2022).